Journal of Fluids and Structures (2001) **15,** 351–364
doi:10.1006/jfls.2000.0333, available online at http://www.idealibrary.com on IDEAL®

OBSERVATIONS OF BUBBLE SELF-ORGANIZATION IN LASER-MATTER INTERACTIONS

S. LUGOMER

Ruder Bošković Institute, Bijenička c. 54, 10002 Zagreb, Croatia

Bubbles generated in laser–metal interactions (LMI) at the transition from planar-to-volume boiling behave like hard (and soft) spheres. Micrographic analysis indicates that the surface layer of vaporizing metal, which comprises small microscale bubbles, behaves like a two-dimensional granular system. Bubble collision leads to bubble self-organization which changes with laser power density Q_p, and falls into (i) the kinetic regime, (ii) the clustering regime, or (iii) the regime of inelastic collapse (when bubbles form chain-like clusters), in analogy with the results of numerical simulations of hard-sphere dynamics. At a certain power density, shock waves that travel over the surface become strong enough, so that the system of bubbles behaves like horizontally and vertically shaken granular material. Since bubbles in the vibrational process are decelerated, hydrodynamic forces deform them, causing them to stay coalesced after the collision, forming a cluster with plateau borders, which is actually metal foam. The results presented show the existence of various complexity levels in the self-organization of bubbles, their sensitivity to the variation of interaction parameters, and finally, they indicate some universal features of bubble system dynamics.

1. INTRODUCTION

A SERIES OF STUDIES OF SELF-ORGANIZATION (SO) of various types of entities in laser–matter interaction (LMI), like droplets (Lugomer & Maksimović 1996), vortex filaments (Lugomer 1996, 1998; Lugomer & Maksimović 1997), and bubbles (Lugomer & Maksimović 1999) has shown that various types of patterns of every entity can be generated. It has also been shown that these patterns change not only in the morphological sense, but also in the sense of topological complexity, depending (for $\tau = 10$ ns laser pulse) on laser power density Q_p.

In this paper, we consider SO patterns of bubbles generated in LMI at the onset of normal boiling in the terminology of Miotello & Kelly (1995). It is rather surprising that their patterns strongly resemble the patterns of hard spheres, generated in a collision process.

Gas-phase nucleation that starts inside a surface layer (or slightly below it) does not appear over the whole interaction space (as usually assumed) but at certain zones only; the change of laser power density leads not only to a change of bubble density, but also to different types of collision processes. This paper seems to be the first one that shows that the beginning of volume vaporization in laser–matter interactions (LMI) is a complex process, which belongs to different types of bubble dynamics in different regions (inside the interaction space). These basins of dynamics comprise different types of bubble SO, which includes regular, irregular, and chaotic structures. In some cases, chain-like, bubble formations were also observed.

In the following, we consider the problem of bubble self-organization in different basins observed under the same laser and experimental conditions on a Ta surface. This paper indicates that these SO processes are very similar to the SO processes of hard (and soft) spheres, but it also raises some questions about this similarity.

0889–9746/01/020351 + 14 $35.00/0

2. EXPERIMENTAL SYSTEM

A series of experiments were performed in order to generate bubbles in the transition regime from planar-to-volume vaporization, to study their spatial organization, the interaction with shock waves, and their dynamics. A Q-switched Nd-YAG laser of $E = 0.3$ J of pulse radiation of 10 ns was used to irradiate the target. The pulse power density Q was varied below (and up to) the volume boiling threshold of 10^8 W/cm^2 by varying the spot size, until bubbles start to appear on the surface. The variation of the spot size caused the change of bubble self-organization.

The tantalum (Ta) plates were mechanically polished and washed in alcohol. Micrographs of laser-treated surfaces were obtained using scanning electron microscopy (SEM), and then were numerically filtered by using the Adobe Photoshop Program. Various details were made visible by changing the recognition level in the program.

3. RESULTS AND DISCUSSION

3.1. Bubble Self-Organization on a Free Vibrating Surface: Small Vibrational Amplitude: $A \approx 0$

A vaporizing surface of metal is exposed to shock waves, acoustic waves, etc., traversing the interaction space in various directions. We first consider the case of bubble dynamics at small laser power density, when the vibrational amplitude A is small or absent, thus transforming the problem into the problem of bubble SO on a free surface at rest.

3.1.1. *Bubble self-organization of type I*

At the laser-induced transition from planar-to-volume vaporization, the Ta surface is covered with bubbles, the distribution of which is pre-dominantly homogeneous or homogeneous-like. [Notice that an ideally homogeneous bubble distribution can hardly be obtained in LMI on a vaporizing metal surface at $T \sim 5000$ K. Homogeneous bubble distribution is more likely to be obtained at (very) small bubble density, like that shown in the upper right part of Figure 1. Such distributions are generated mostly at the very threshold of vaporization by precise adjustment of laser power density.]

Homogeneity in bubble distribution exists in separate basins (inside the laser spot) in which bubble dynamics and self-organization occur independently. Figure 1 (which shows a frozen-in situation after the laser pulse termination) is obtained from the SEM micrograph by numerical filtration under high contrast. High contrast suppresses all unimportant details and background features, showing bubble-like black dots. This bubble formation is not a cluster because particles do not touch each other. In this regime, a system of spheres that begins in an initial state of uniform density with a Maxwellian distribution of velocities experiences several hundred collisions per particle. The system then "cools" as the collisions dissipate the kinetic energy of the initial state (McNamara & Young 1994).

This type of bubble organization may be compared with the organization of hard spheres in two dimensions, obtained in numerical simulation by McNamara & Young (1994). Their numerical simulation performed for the restitution coefficient $r = 0.88$ and the number of collisions $C/N = 400$, $N = 1024$ inelastic discs, showed that the behaviour of bubbles is similar to the behaviour of molecules in the so-called "kinetic regime" [Figure 1(b)], which does not result in clustering.

By a slight reduction of the spot size ($\leq 10\%$), i.e. via an increase in power density, the bubble formation (the SO structure) changed into a periodic wavy-structure shown in Figure 2(a). Since particles are separated, i.e. they do not touch each other, this periodic

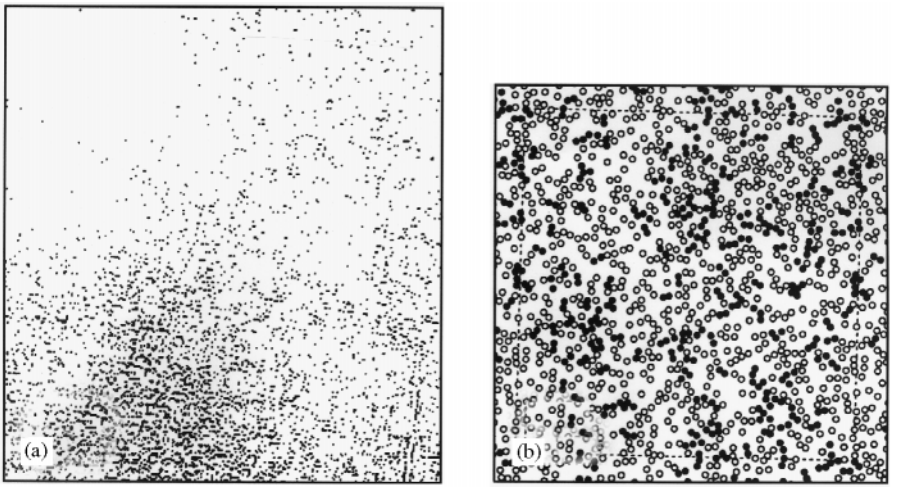

Figure 1. (a) Laser-induced bubble formation on Ta surface in the "kinetic regime". The micrograph was numerically filtered with high contrast, so that bubbles appear as black dots; M $\sim 250\times$ (b) Numerical simulation: the final ($C/N = 400$) "kinetic regime" configuration of $N = 1024$ inelastic discs with $v = \frac{1}{4}$ and $r = 0.99$, the solid discs are all particles that participated in the final 200 collisions of this simulation (from McNamara & Young 1994).

wavy-like SO of bubbles also belongs to the "kinetic regime". It may be compared with the wavy formation of hard spheres under periodic boundary conditions, and under the same initial conditions as above, i.e. homogeneous bubble density, homogeneous temperature, and isotropic and homogeneous velocity distribution. The behaviour of such a system, consisting of 20 000 spheres, was numerically simulated by Goldhirsch & Zanetti (1993), supposing the Maxwellian velocity distribution. They have shown that the equipartition of energy is prominent at early stages, whereas a typical scale corresponding to the wavevector $k = \pi$ is observed at later stages (corresponding to the predominance of the slowest shear mode in the system). Figure 2(b) represents a typical result of the numerical simulation of the mass distribution of the disks after a long enough time. The size of such a system is less than $\ell/(1 - \tilde{r}^2)^{1/2}$, i.e. less than ℓ/r, where ℓ is the mean free path of a sphere and r is the restitution coefficient (Goldhirsh & Zanetti 1993). Figure 2(b) shows density nonuniformity but no discernible clusters, and therefore belongs to a kinetic regime of dynamics. This figure can favourably be compared with our figure [Figure 2(a)], which shows a system of bubbles on a Ta surface with a periodic distribution.

3.1.2. *Bubble self-organization of type II*

By increasing the laser power density by a stepwise reduction of the spot size by $\leq 10\%$, one can observe the change in the bubble formation and deviation from the "kinetic regime". Bubbles are no longer separated but touch each other at a point, and give rise to rectangular cells, as shown in Figure 3(a). This figure shows the bubble formation, which may be compared with the formation of spheres obtained by numerical simulation of the "clustered regime". If the state of uniform density of spheres is unstable in a cooling "granular" medium, clusters start to form throughout the gas. Clustering occurs when the density of the granular medium spontaneously becomes nonuniform. This was demonstrated for a slightly different restitution coefficient ($r = 0.8$), and for the same value of N ($N = 400$) by McNamara & Young (1994). The transition from the "kinetic regime" to the

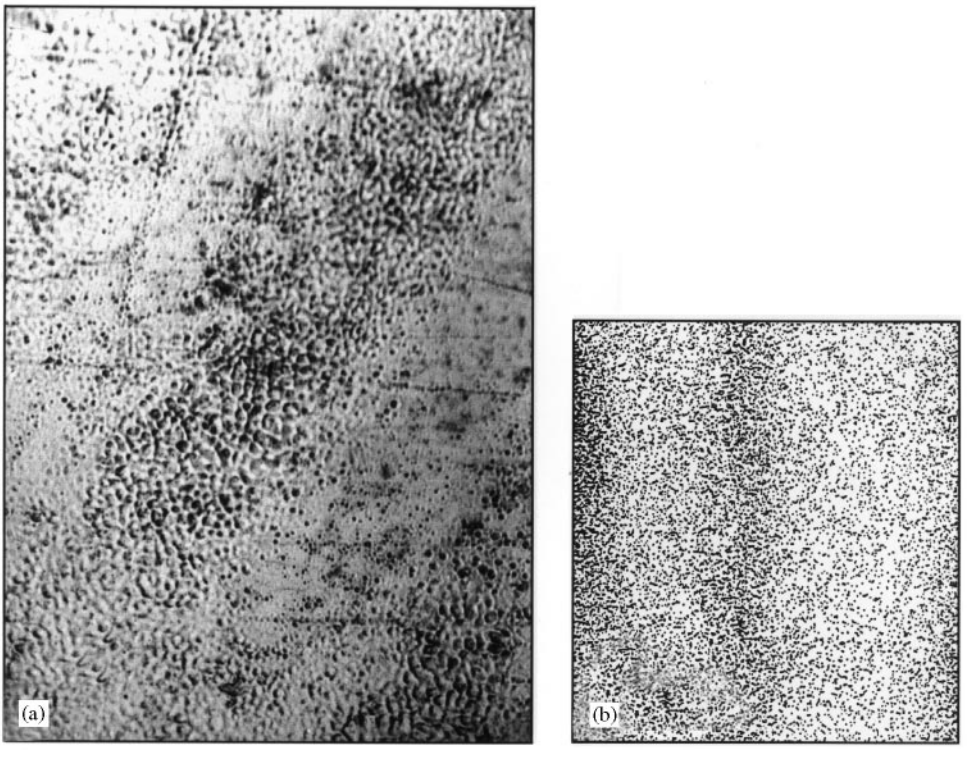

Figure 2. (a) Laser-induced bubble formation on Ta surface in the "clustering regime" under periodic boundary conditions. (b) Numerical simulation: particle following 500 collisions per particle. Here $\tilde{e} = 0.98$, and the number of particles is 20 000 (from Goldhirsh & Zanetti 1993).

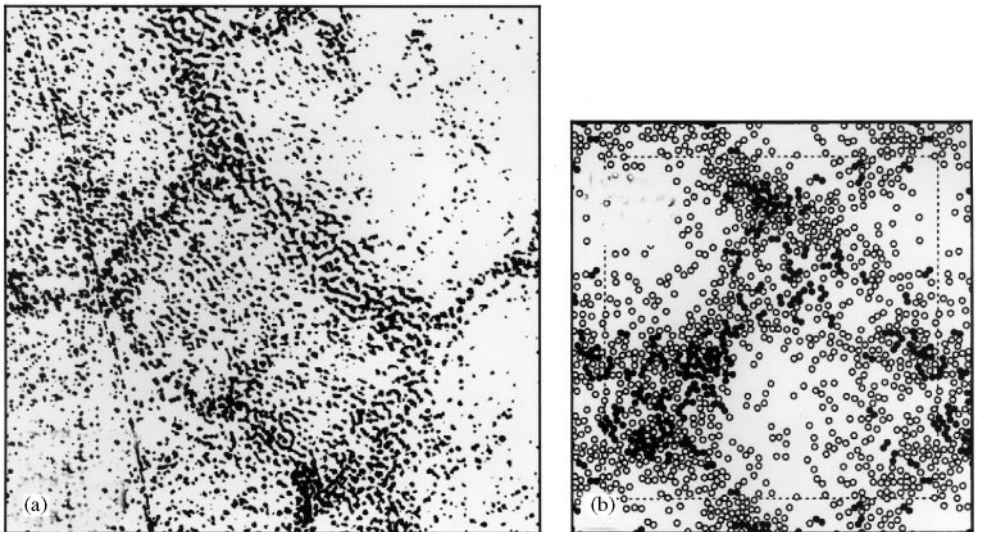

Figure 3. (a) Laser-induced bubble formation on Ta surface in the "clustering regime" with a rectangular 2-D lattice; M $\sim 250\times$ (b) Numerical simulation: the final ($C/N = 400$) "clustered regime" configuration of $N = 1024$ inelastic discs with $v = \frac{1}{4}$ and $r = 0.8$; the solid discs are all particles that participated in the final 200 collisions of this simulation. (from McNamara and Young 1994).

"clustered regime" is a long-wavelength instability described by kinetic theories. Clusters cannot form in domains too small to allow linearly unstable waves. The bubble clustering observed on a Ta surface, shown in Figure 3(a), can be compared to the clustering in Figure 3(b) obtained by numerical simulation (McNamara & Young 1994), for the granular medium.

3.1.3. *Bubble self-organization of type III*

Further increase in laser power density results in a new type of bubble self-organization, which is different from that described above. Bubbles are grouped into large clusters in which spheres (discs) are in "solid" contact and stay permanently in this position after collisions. Figure 4(a) shows two black curves (chains) of bubbles in permanent contact. This figure can be compared with the numerically generated chain-like clusters of McNamara & Young (1994), shown in Figure 4(b), clusters were obtained on 40 000 inelastically colliding particles, clustering per particle, and the average area occupied by particles was 0.05. A new qualitative phenomenon that occurred was called the inelastic collapse. McNamara & Young (1994) showed that inelasticity could lead to an infinite number of collisions occurring at a finite time. This type of bubble self-organization appeared if the system size was larger than ℓ/ε. In the 1-D case, such a collision sequence made particles "stick" together in close contact, with no relative motion. Such a situation was generated with $r = 0.6$ and $C/N = 68.3$. The inelastic collapse in the 2-D case produced dense chain-like formations inside clusters (Petravić *et al.* 1993).

The relationship between the inelastic collapse and the phenomenon of clustering, which indicates the breakdown of ordinary hydrodynamics, needs clarification. One plausible scenario is that, once the system forms clusters, the occurrence of the inelastic collapse exceeds a critical value. Another scenario assumes all clusters to be transient, which must eventually terminate in either the inelastic collapse or the formation of shear bands (Jaeger *et al.* 1996).

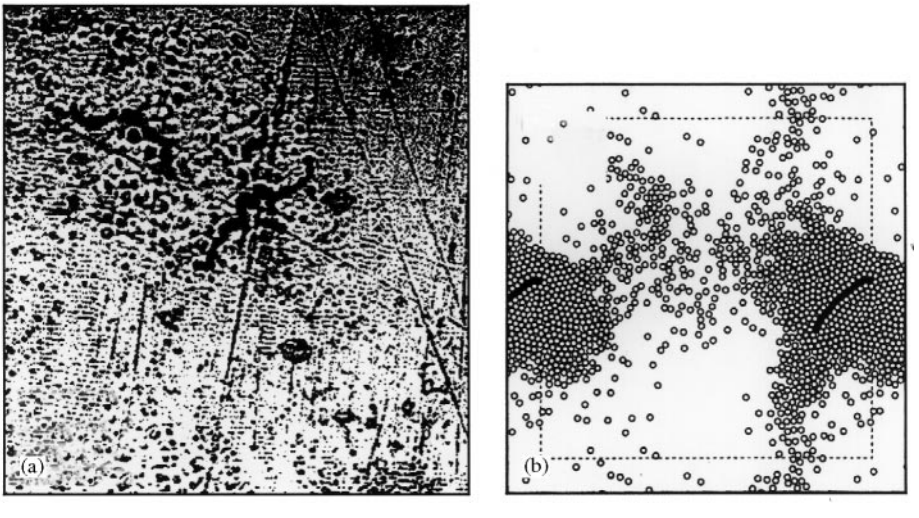

Figure 4. (a) Laser-induced bubble formation on Ta surface in the "collapsed regime". The chain-like formations of bubbles in contact are clearly seen. Notice the excitation of Faraday waves around the bubble cluster, which are characteristic of the boiling surface. (b) Numerical simulation: the final ($C/N = 68.3$) "collapsed regime" configuration of $N = 1024$ inelastic discs with $v = \frac{1}{4}$ and $r = 0.6$; the solid discs are all particles that participated in the final 200 collisions of this simulation. (from McNamara & Young 1994).

3.2. Bubble Dynamics of a Free Vibrating Surface: Large Vibrational Amplitude: $A \neq 0$

With the reduction of the spot size, laser power density increases so that shock waves generated in LMI become more intense. When their intensity becomes large enough to influence bubble dynamics, some new characteristics in the bubble self-organization set in.

A vaporizing surface containing bubbles is excited by shock waves, and behaves as a free surface of vibrated liquid, similarly to a free vibrating surface of granular material. It exhibits several wave phenomena, as well as more complex irregular (and possibly chaotic) states (Jaerger *et al.* 1996; Pak & Behringer 1993), i.e. it resembles the system of hard spheres.

3.2.1. *Inelastic collapse of bubbles caused by travelling waves*

The large vibrational amplitude of a vaporizing surface (which contains bubbles), causes the surface oscillatory motion, which can be expressed as

$$Z_0'(f) = A(x)\sin(2\pi ft), \tag{1}$$

where f is the frequency. The amplitude A can have a spatial modulation of the form

$$A(x) = A_0[1 - B\cos(2\pi x/L)], \tag{2}$$

as supposed by Gallas *et al.* (1992).

The different waves arising in this oscillatory system can be either travelling or standing (when hopping is weak or nonexistent). Also, subharmonics and their superposition occur, which is strikingly similar to Faraday instabilities in ordinary liquids (Fouve *et al.* 1992).

Different types of bubble clusters have been observed. This indicates that self-organized patterns of bubbles are a consequence of (surface) transient waves, which generate clusters that change in space–time. Consequently, different clusters have a (slightly) different shape at the moment of pulse termination. The most frequently observed clusters are quasi-hexagonal bubble clusters shown in Figure 5(a, c), which are a consequence of oscillation-induced parametric wave patterns of spheres. They may be interpreted in the spirit of Mello *et al.* (1994, 1995), Taguchi (1992), Gallas *et al.* (1992) and Bourzutschky & Miller (1995) for the convection in vertically oscillated granular material, as well as in the spirit of Pak & Behringer (1993) for the patterns generated by surface waves. Namely, the internal structure of clusters reminds one of the structure characteristic of oscillatory convection patterns. On the other hand, their contour (polygonal) is shaped by the fronts of random surface waves, as shown in the corresponding schematic reconstructions in Figure 5(b, d). It is seen that the wave fronts of the surface waves form quasi-regular clusters in addition to (besides) hexagonal ones.

In our view, these patterns formed on a vaporizing Ta surface may be assumed to be patterns formed in the presence of a series of random (surface) waves generated simultaneously by vertical and horizontal excitation. Let us now look at two characteristics of clusters: (i) bubble size distribution and (ii) bubble–bubble boundary.

(i) *Bubble size distribution inside a cluster*

Magnification of a bubble cluster indicates that larger bubbles are located at the centre of the cluster, whereas smaller ones are on its periphery (Figure 6). This can also be observed in quasi-hexagonal clusters in Figure 5. Such a size separation of bubbles is typical of a vibrated system of spheres. When granular materials are vibrated (or shaken), particles of different sizes tend to separate with the largest particles moving to the centre and to top,

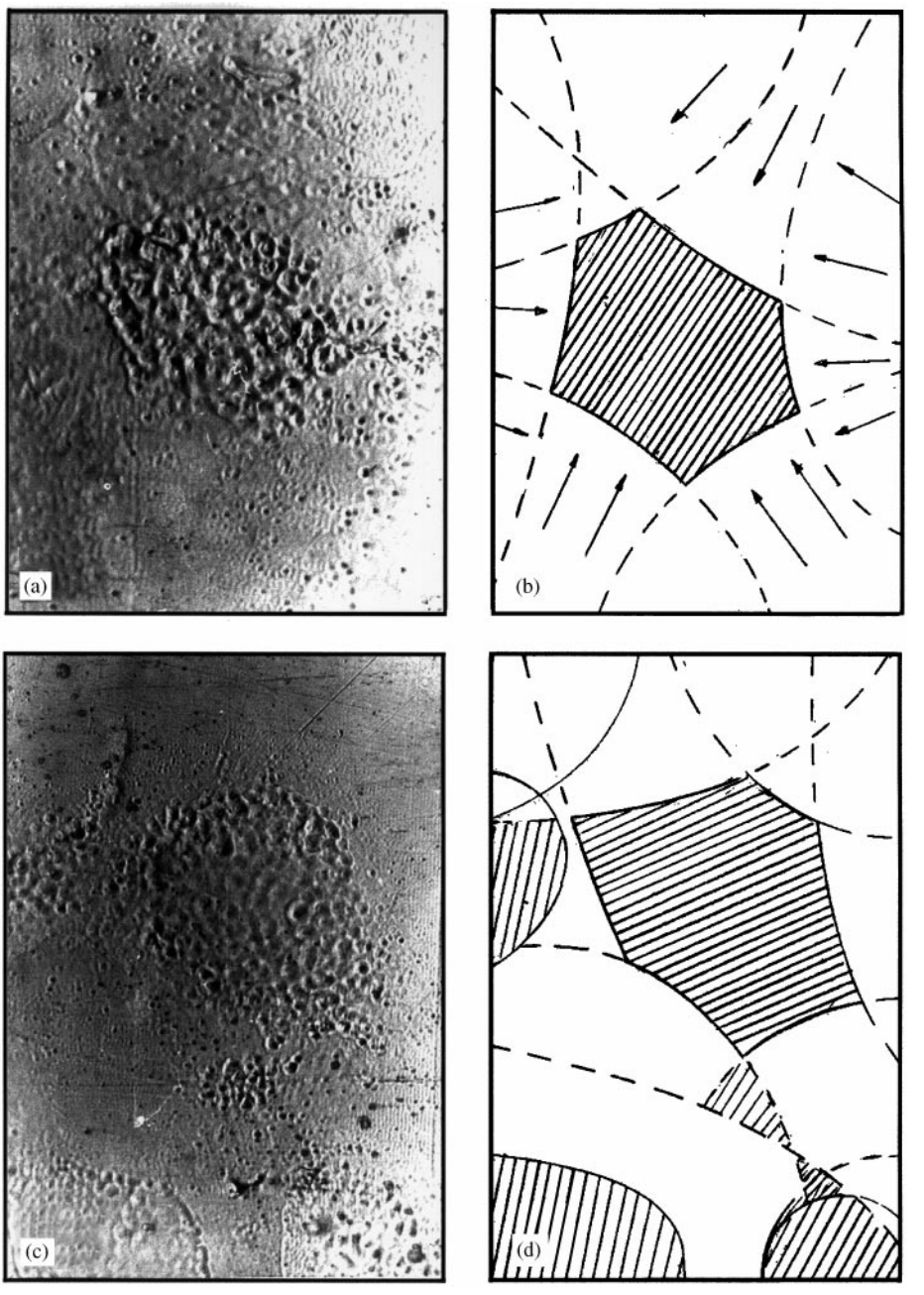

Figure 5. Laser-induced quasi-hexagonal bubble formation on Ta surface, formed by horizontal + vertical oscillations of vaporizing surface caused by shock waves. (a) Micrograph showing a relatively regular hexagonal bubble cluster: $M \sim 400\times$ (b) Reconstruction (schematic) of Figure (a), showing random surface waves whose fronts form the bubble contour. (c) Micrograph showing quasi-regular hexagonal cluster as well as some clusters of chaotic shape; $M \sim 400\times$. (d) Reconstruction of Fig. (c) showing the fronts of random surface waves.

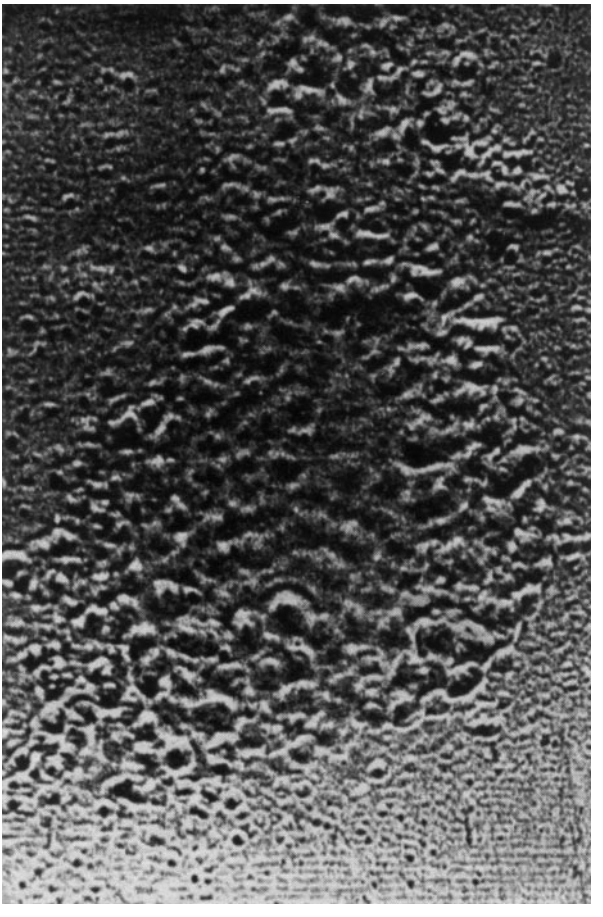

Figure 6. Bubbles in the cluster are in contact along lines or planes (plateau borders), thus giving rise to metal foam M $\sim 500\times$. The lower part of the figure shows Faraday waves.

independent of their density. Continuing the comparison of bubbles with granular materials, several mechanisms have been considered with such size separation, but none of them can be *a priori* identified as responsible for bubble size separation.

In vertically shaken systems, however, experiments have shown a direct link between convection and size separation. Large spheres become entrained in the upward connection flow, whereas smaller ones stay at the periphery. This is also an argument in favour of the presence of vertical vibrations of the vaporizing surface.

(ii) *Bubble–bubble boundary inside a cluster*: *metal foams*

Another important characteristic of bubble clusters shown in Figures 5 and 6 is that bubbles are in contact with their neighbours not at a single point, but along lines (or more precisely, along planes), thus having a polyhedral form. Since bubble clusters of polyhedral form are foam, the clusters in Figures 5 and 6 are metal foams. Their generation may be understood as a consequence of the fact that bubbles start to behave as soft spheres. This is because strong horizontal and vertical shaking reduces their horizontal velocity and decreases the Weber number. At decreasing velocity, bubbles behave not like hard but like soft spheres. As a consequence, hydrodynamic forces cause deformation of bubble pairs on

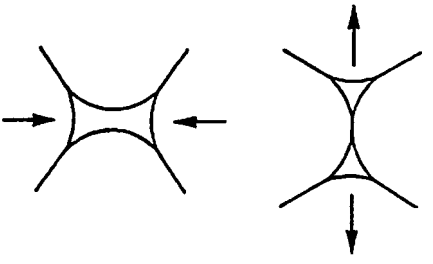

Figure 7. Examples of topological processes involving finite plateau borders. The intermediate state which has a four-fold border can be stable under certain circumstances (from McNamara & Young 1993).

collision, so that bubbles coalesce after the collision event. A cluster of bubbles that suffers deformation and collisional coalescence makes foam. Foam polyhedrons (ranging from six- to eight-sided ones) appear to be quasi-regular, rather than regular. In contrast to ideal cases, a foam polyhedron does not have a perfectly ordered (honeycomb) structure of equal cells.

Foam consists of cells, surrounded by sides of constant thickness (after an initial draining process), each side being of constant curvature. The sides meet at plateau borders (Weaire 1992; Weaire *et al.* 1993) whose size depends on the pressure maintained in the liquid network of sides/borders. The curvature of the borders and sides depends on the pressure differences across them. This is in agreement with the elementary conditions of equilibrium, which express the balance of pressure and surface tension. The surface tension or energy of the films is the key to the stability of the whole structure. According to Weaire (1992), a mechanism is available by means of which the surface energy may be lowered indefinitely. The mechanism acts as the transfer of gas between cells; in most cases, this is a slow process for the foam. From another point of view, this is simply the diffusion of gas through liquid films in response to the difference in pressure between the cells on either side, and proportional to it (Weaire *et al.* 1993). It causes large cells to grow by coalescence at the expense of small ones by coalescence. The resulting evolution is expressed as topological changes of various kinds, some of which are shown in Figure 7.

All bubbles do not show an ideally spherical top, but a top whose shape is intermediate between a spherical and a polygonal shape. This may be understood as a consequence of the variation of amount of the liquid in the foam. Weaire (1992) and Weaire *et al.* (1993) observed the wet foam with spherical bubbles on top, separated from the dry polyhedral foam underneath by a very sharp boundary. The boundary moves down as the extra fluid is drained by gravity. They have shown that the boundary velocity is proportional to the square-root of the liquid flow rate, which they justified using single-scale arguments involving viscous Poiseuille flow along linear channels on the edge of the polyhedral bubbles (called the plateau borders). In Poiseuille flow, the fluid sticks on the walls and moves fastest in the middle of the channels. The rate of flow is proportional to the square of the channel cross-section.

4. DISCUSSION

The foregoing results open some interesting and important questions. Being rather surprising, they indicate an analogy in the collective behaviour of solid spheres and of microbubbles, i.e. the behaviour of granular material. However, many questions arising from this analogy cannot be answered presently. To answer these questions, let us first consider the

bubble characteristics as well as the collision process of such spheres.

4.1. Hydrodynamic Aspect: Bubble Characteristics

It is well known that small bubbles can be approximated by spheres, and that the entire bubble surface may become rigid (Maruvada & Park 1996). Many studies of bubble–bubble collision have shown that the behaviour of bubbles depends on the Reynolds number, Re, and the Weber number, We (Tsao & Koch 1997):

$$\mathrm{Re} = \frac{\rho U \sigma}{\mu}, \qquad \mathrm{We} = \frac{\rho U^2 \sigma}{\Gamma}, \tag{3}$$

where ρ and μ are the density and viscosity of the liquid, U and σ are the velocity and equivalent size of the bubble, and Γ is the surface tension of the liquid/air interface (Chesters & Hofman 1982). Tsao & Koch (1997) have found that bubbles for $\mathrm{We} \ll 1$ and $\mathrm{Re} \gg 1$ collide and coalesce on contact. The hydrodynamic force is sufficient to cause a significant deceleration of bubbles required to make contact. At moderate values of We, bubbles begin to deform before the gap thickness becomes very small. Thus, it is possible that the film between the two deformed bubbles becomes large enough to allow the inertial pressure in the film to arrest the bubbles motion before contact. The studies of stationary bubble clouds indicate that the two bubbles will bounce if the We number exceeds some critical value ($\mathrm{We}_{\mathrm{initial}} = 0{\cdot}28$ for bubbles of $\sigma = 0{\cdot}5$–$0{\cdot}7$ mm). At high We numbers, the bubbles bounce, as observed by Tsao & Koch (1997) and others.

The system of bubbles forming an elastic solid of hard spheres shows the "rigidity loss transition" and many other interesting phenomena, which have been studied by Bolton & Weaire (1990), Hutzler *et al.* (1998) and others. Recent studies have shown that even soap bubbles behave as a 2-D system of hard spheres for a small value of the liquid fraction, ϕ ($\phi_{\mathrm{critical}} \approx 0{\cdot}16$), where ϕ_{c} is identified as the density of random packing of hard discs (Hutzler *et al.* 1998).

Very small laser-generated bubbles (micron scale) may be regarded as rigid spheres, and their collision on the short time scales (large velocity) can be approximated by the behaviour of hard spheres. According to Maruvada & Park (1996), small bubbles behave according to the criterion $\sigma/L \ll 1$, where σ is the bubble size and L is the size of the system (the spot diameter in this case). For laser-generated bubbles σ is 10^{-6} m, the spot size L is $2\text{–}3 \times 10^{-3}$ m (or more), which gives $\sigma/L \ll 1$, so that bubbles can be regarded as small and hard spheres. If the bubble deformation is allowed in the collision process, the soft-sphere behaviour is more appropriate.

4.2. Conceptual Framework of Bubble Self-Organization: Collisional Process in a 2-D Granular System

We assume a bubble to be a sphere (or a disc in two dimensions), and a thin vaporizing metal surface to be (homogeneously) covered with bubbles as a granular system.

It is known that granular materials act as fluids, solids, and gases depending on how they are excited (Lubkin 1995). At present there is no comprehensive understanding of the fluid-like state of granular materials (of either hard or soft spheres), let alone the cross-over between fluid-, solid- and gas-like behaviour. The fluid-like state in particular arises from a highly nonlinear response to external vibrations. Concepts from ordinary hydrodynamics or statistical mechanics fail for granular media, because the thermal energy is irrelevant and all collisions are inelastic, which gives rise to the problem of an appropriate theoretical

framework. Granular materials behave differently from continuous media (such as rigid, elastic, or viscous bodies). This difference is due to the fact that granular materials behave in two distinct ways: as a set of particles and as continuous media (Taguchi 1992).

Hard and soft spheres: Fluctuations in a system of spheres lead to inelastic collisions and dynamics, which can be described (Goldhirsch & Zanetti 1993, Petravić 1993; McNamara & Young 1994) by the system of equations

$$\rho \frac{\mathrm{D}\mathbf{V}}{\mathrm{D}t} = -\nabla\mathbf{P}, \tag{4}$$

$$\frac{2}{3}\rho \frac{\mathrm{D}T}{\mathrm{D}t} = -\nabla\mathbf{Q} - \mathrm{tr}(\mathbf{PD}) - \gamma, \tag{5}$$

$$\rho = -\nabla(\rho\mathbf{V}), \tag{6}$$

where $\mathrm{D}/\mathrm{D}t$ is the material derivative, ρ is the mass density, T the temperature of the sphere, V the velocity field, $\mathbf{D}$ the symmetrized velocity gradient tensor, $\mathbf{P}$ the stress tensor, $\mathbf{Q}$ the heat flux, and γ the rate of energy loss due to inelastic collisions.

The above constitutive relations are valid for dilute granular gases where the coefficient of restitution $\tilde{r}$ is not too small. The hydrodynamic stress tensor is given by (Goldhircsh & Zanetti 1993)

$$\mathbf{P} = -P_h\mathbf{I} - 2\mu(\mathbf{D} - \frac{1}{3}\mathrm{dir}\, v\mathbf{VI}). \tag{7}$$

Here $\mathbf{I}$ is the unit tensor, P_h the pressure, and μ the viscosity; $\mathbf{Q} = k\nabla T$; $P_h = a\rho T$, and the viscosity is $\mu = b\sigma\rho_s T^{1/2}$, the heat conductivity $k = c\sigma\rho_s T^{1/2}$, and $\gamma(\mathrm{d}\rho_s/\sigma)T^{3/2}$. σ is the diameter of the particle, ρ_s the density of spheres, a, b, and c are constants, while $\alpha = f(r)$, where r is the coefficient of normal restitution. Since the energy dissipated in a single collision is proportional to $1 - \tilde{r}^2$, the coefficient of normal restitution is taken as $r = 1 - \tilde{r}^2$ (Goldhircsh & Zanetti 1993).

This simulation of the dynamics of the system of spheres is based on a comparison between the mean free path of the sphere ℓ, the total cross-section diameter for collision σ, the particle density N, and the restitution coefficient r.

Since the collision of spheres occurs at the surface only, i.e. in 2D space, the spheres may be substituted (in the model) by discs. The difference between hard and soft spheres is introduced through the collision potential ϕ, which enters into the pressure tensor $\mathbf{P}$ through the probability density function f (Petravić 1993).

The potential ϕ is the Lennard–Jones potential, which is truncated for hard spheres (Petravić 1993) as

$$\phi^{\mathrm{hard}} = \begin{cases} 4\varepsilon\left[\left(\dfrac{\sigma}{r'}\right)^{12} - \left(\dfrac{\sigma}{r'}\right)^{6}\right] + \varepsilon & \text{for } r' < \sqrt[6]{2}\sigma \\ 0 & \text{for } r' < \sqrt[6]{2}\sigma \end{cases}, \tag{8}$$

and for soft spheres as

$$\phi^{\mathrm{soft}} = \begin{cases} 4\varepsilon\left[\left(\dfrac{\sigma}{r'}\right)^{12} - \left(\dfrac{\sigma}{r'}\right)^{6}\right] + \varepsilon & \text{for } r' < \sigma \\ 0 & \text{for } r' < \sigma \end{cases}, \tag{9}$$

where ε is the depth of the potential well that controls the energy of interaction.

The collision of soft discs takes place not in the point but over a finite path. The point particle moves through the scattered particles during the collision, and the kinetic part of the pressure tensor consists of the free streaming part between the collisions and of the part during the collision. At $T^* = 1 (T^* = k_B T/\varepsilon =$ reduced temperature) the kinetic contribution of collisions is small compared with the contribution of free trajectories between the collisions, because the repulsive force is sufficiently strong not to allow the point particle to spend much time within the scatters. The motion of the particle between the collisions obeys the same equation of motion for hard and soft discs. Therefore, the dependence of the kinetic part of the normal stress difference and the off-diagonal element of the pressure tensor on the shear rate for soft disks resembles the dependence for hard discs. Petravić (1993) has shown that the behaviour of the pressure tensor for soft discs is similar to the behaviour for hard discs, at least in the range of shear rates $\gamma^* \leq 3$ ($\gamma^* = m\gamma\sigma/p = \gamma\sigma\sqrt{m/\varepsilon} =$ reduced shear rate): the normal stress difference is negative for $\rho^* = 0{\cdot}4$ [$\rho^* = \rho\sigma^2 =$ reduced number density), and becomes negative for $\gamma^* > 1{\cdot}5$, for $\rho^* = 0{\cdot}1$. However, the collision impulse for the finite force is smaller than the impulse for infinitively hard discs, and this is the main reason that the potential part of the pressure tensor has a smaller absolute value for soft discs, than for hard discs. In a qualitative sense, three regimes of collision of hard and soft discs can be distinguished (McNamara & Young 1994): (i) the "kinetic regime", (ii) the "clustering regime", (iii) the regime of "inelastic collapse".

The above theoretical outline relating to the self-organization of hard and soft spheres can be a tentative framework for the concept of self-organization of a 2-D microbubble system.

We have observed that the bubble dynamics changes with the change of the spot size (laser power density). Their self-organization also changes, in passing from one to another type of organization, which strongly reminds one of the above regimes of collision of hard spheres.

The question of how the variation of laser power density influences the bubble collision process is not a simple one. We assume that the influence of the increased energy deposition rate into the target surface (associated with increased Q_p) does not result in an increase in temperature (of the vaporizing surface), but in a larger bubble nucleation rate and consequently, in larger bubble density. In addition, this influence occurs through a change in the number of collisions and, finally, through a change of the restitution coefficient. To our knowledge, the connection (relation) between Q_p and the above parameters has not been studied yet, and it is presently unknown.

Another question that follows relates to the shear rate γ^* and its dependence on Q_p. The influence of the shear rate γ^* on the onset of the "inelastic collapse" (the case when the particle cannot "bounce off"), for a system of hard and soft spheres was studied by Petravić (1993).

According to Petravić (1993), when shear is present, the solution implies that the magnitude of the radial component of momentum is different before and after the collision. The point particle has a larger radial component after the collision in the quadrants where the radial component of streaming velocity is negative, and a smaller radial component where the radial component of streaming velocity is positive. In the former case, the impulse is larger, whereas in the latter case it is smaller, than in equilibrium. The dependence of the impulse on the polar angle of the momentum and on the coordinates of the collision point can qualitatively explain the dependence of the potential part of the pressure tensor on the shear rate, and the dependence of the potential of the latter on density and the shear rate as separate parameters. A similar dependence of the potential part of the pressure tensor on the shear rate for soft disks using the Lenard–Jones potential truncated at $r' = \sigma$ gives confidence in the correctness of the collision law for hard discs (Petravić 1993).

The solution of thermostated collision with shear shows that, for the reduced shear rate $\gamma^* > 4$, such collisions may occur when the moving particle cannot "bounce off" after the collision, but stays bound infinitely to the scatterer. These "forbidden" collisions have the same origin as the artificial string phase observed in the strongly sheared soft disc systems. The limit $\gamma^* = 4$ can be interpreted as the limit of applicability of the linear streaming velocity profile. The actual probability distribution of the polar angle β of the collision depends on density. For very low density, $\rho^* \ll 0{\cdot}1$, collisions are confined to points very close to the top and bottom of the scatterer because of the nearly horizontal trajectories in the vicinity of the scatterer. Therefore, for such low densities, the "forbidden" collisions may occur, for the first time, at shear rates higher than $\gamma^* = 4$, and the limit of applicability of the linear profile thermostat may be density dependent (Petravić 1993).

Since the bubble density is proportional to Q_p, it is possible that γ^* also depends on Q_p, but the nature of this dependence is not presently known.

5. CONCLUSION

Bubbles generated in laser–metal interaction at transition from planar-to-volume vaporization, behave like a 2D-system of rigid or semirigid spheres that undergo collision dynamics, which reminds one of the behaviour typical of granular materials.

On a very short time scale ($T = 10$ ns), the bubble velocity is high, so that deceleration (which leads to their deformation) does not occur. Consequently, they collide like hard spheres. The bubble self-organization (which stays frozen-in after the pulse termination) reveals three dynamic regimes, called by analogy with the system of hard spheres: (i) the kinetic regime, (ii) the clustering regime, and (iii) the regime of inelastic collapse. The regime of bubble self-organization varies with changes of laser power density Q_p. The increase of Q_p by $\leq 10\%$ step (in the state of planar vaporization) causes a change of the collisional regime from the kinetic, to the clustering regime, and finally to the regime of inelastic collapse. Bubble self-organization in each of these regimes has been compared with the corresponding SO structure of hard spheres, generated by numerical simulation. When the shock wave intensity becomes large enough to affect the bubble velocity, bubbles behave as vertically and horizontally shaken (vibrated) granular material. These vibrations cause a decrease of the bubble horizontal velocity, which leads to the situation when hydrodynamic forces deform bubbles before collision. Bubbles then behave like soft spheres, which leads to their coalescence after collision, and to the formation of metal foam.

The above results have surpass a mere (practical) consideration of laser–matter interactions. They indicate the existence of various complexity levels in the self-organization of bubbles on a small space–time scale. The variation of self-organization with the variation of power density and connection to the "internal" control parameters (number of collisions, restitution coefficient, dimension remains to be elucidated.

ACKNOWLEDGEMENTS

The author is grateful to Dr K. Furić, Ruder Bošković Institute, for numerical filtration of micrographs. The author is also grateful to Dr J. Petravić, Laboratoire de Cheímie-Physique des Materiaux Amorphes, Université de Paris-Sud, Orsay, for critical reading of the manuscript.

References

Bolton, F. & Weaire, D. 1990 Rigidity loss transition in a disordered 2D froth. *Physical Review Letters* **65**, 3449–3451.

Bourzutschky, M. & Miller, J. 1995 "Granular" convection in a vibrated fluid. *Physical Review Letters* **74**, 2216–2219.
Chesters, A. K. & Hofman, G. 1982 Bubble coalescence in pure liquids. *Applied Scientific Research* **38**, 353–360.
Fouve, S., Kumar, K., Laroche, C., Beysus, D. & Garrabos, Y. 1992 Parametric instability of a liquid–vapor interface close to the critical point. *Physical Review Letters* **68**, 3160–3163.
Gallas, J. A. C., Herrmann, H. J. & Sokolowski, S. 1992 Convection cells in vibrating granular media. *Physical Review Letters* **69**, 1371–1374.
Goldhirsch, I. & Zanetti, G. 1993 Clustering instability in dissipative gases. *Physical Review Letters* **70**, 1619–1622.
Hutzler, S., Weaire, D. & Crawford, R. 1998 Convective instability in foam drainage. *Europhysics Letters* **41**, 461–465.
Jaeger, H. M., Nagel, S. R. & Behringer, P. R. 1996 The physics of granular materials. *Physics Today* **49**, 32–38.
Lubkin, G. 1995 Oscillating granular layers produce stripes, squares, hexagons. *Physics Today* **48**, 17–19.
Lugomer, S. & Maksimović, A. 1996 Laser-induced bursts of subsurface liquid Mo at transition from planar to volume vaporization: ballistic and percolation surface aggregation of ejected particles. *Vacuum* **47**, 1053–1059.
Lugomer, S. 1996 Observation of laser-induced microscale knotted and unknotted vortex filaments on vaporizing tantalum surface. *Physical Review* **B54**, 4488–4491.
Lugomer, S. & Maksimović, A. 1997 Solitons on vortex filaments generated by ns laser pulse on metal surface. *Journal of Applied Physics* **82**, 1374–1383.
Lugomer, S. 1998 Observation of laser-induced cellular organization of vortex filaments, spatial period doubling and transition to chaos. *Journal of Applied Physics* **83**, 510–517.
Lugomer, S. & Maksimović, A. 1999 Laser-induced bubble formation and collapse in a nonlinear Rayleigh—Taylor unstable interface in a thin layer of molten metal. *Physics Letters A* **251**, 303–310.
Maruvada, S. R. K. & Park, C. W. 1996 Retarded motion of bubbles in Hele–Shaw cells. *Physics of Fluids* **8**, 3229–3233.
Miotello, A. & Kelly, R. 1995 Critical assesment of thermal models for laser sputtering at high fluences. *Applied of Physics Letters* **67**, 3537–3537.
Mello, F., Umbanhowar, P. & Swinney, H. L. 1994 Transition to parametric wave patterns in a vertically oscillated granular layer. *Physical Review Letters* **72**, 172–175.
Mello, F., Umbanhowar, P. & Swinney, H. L. 1995 Hexagons, kinks, and disorder in oscillated granular layers. *Phyisal Review Letters* **75**, 3838–3841.
McNamara, S. & Young, W. R. 1994 Inelastic collapse in two dimensions. *Physical Review E* **50**, R28–R31.
Pak, H. K. & Behringer, R. P. 1993 Surface waves in vertically vibrated granular materials. *Physical Review Letters* **71**, 1832–1835.
Petravić, J., Isbister, D. J. & Morriss, G. P. 1993 Sheared Lorentz gas attractor. *Journal of Statistical Physics* **48**, 425–434.
Petravić, J. 1993 Some Properties of the Lorentz Gas Attractor, Ph.D. Thesis, University College, The University of New South Wales, Australian Defence Force Academy.
Taguchi, Y. 1992 New origin of a convective motion: Elastically induced convection in granular materials. *Physal Review Letters* **69**, 1367–1370.
Tsao, H. K. & Koch, D. L. 1997 Observations of high Reynolds number bubbles interacting via a rigid wall. *Physics of Fluids* **9**, 44–56.
Weaire, D., Pittet, N., Hutzler, S. & Pardol, D. 1993 Steady-state drainage of an aqueous foam. *Physical Review Letters* **71**, 2670–2673.
Weaire, D. 1992 Some lessons from soap froth for the physics of soft condensed matter. *Physica Scripta* **T45**, 29–33.